ROTORCRAFT SHIPBOARD LANDING GUIDANCE USING MPPI TRAJECTORY OPTIMIZATION

Vinodhini Comandur
vinodhini@gatech.edu
Ph.D. Student

J. V. R. Prasad
jvr.prasad@ae.gatech.edu
Professor

School of Aerospace Engineering,
Georgia Institute of Technology
Atlanta, GA, U.S.A.

Abstract

With shipboard launch and recovery operations remaining a challenge, there is a continuing emphasis to determine pilot assist functions in order to reduce pilot workload arising from handling the effects of ship air wake turbulence, random ship motion and degraded visuals associated with this task. This paper is an extension to previous work which investigated the use of Model Predictive Path Integral (MPPI) approach, a stochastic optimal control method, for trajectory guidance during shipboard landing. With the objective of developing a real-time guidance solution, this paper focuses on understanding the effect of the performance measure and parameters associated with the method by using a linear model for prediction and a nonlinear model as a representation of the actual vehicle. First, in continuation with an earlier paper, a simple study is conducted by including yaw attitude constraint during shipboard landing using a six degrees-of-freedom linear model of the helicopter in the MPPI method. Next, a test is conducted where a linear model is used in the MPPI algorithm to predict the helicopter behavior for the entire landing with a nonlinear model serving as the truth model. Lastly, the effect of prediction window on MPPI performance is investigated. The paper concludes with key observations and inferences gained in this study.

1. NOTATION

A	State matrix
B	Control or Input matrix
C	Output matrix
F	Weighting function
J	Performance measure or index
M	Number of random control vectors or trajectories
p	Body roll rate (rad/s)
Q	Error weighting matrix
q	Body pitch rate (rad/s)
R	Control weighting matrix
r	Body yaw rate (rad/s)
t	Time (s)
u	Control input vector (percent)
u_b	Helicopter body velocity along body x-axis (ft/s)
u_m	Initial guess for control input
v_b	Helicopter body velocity along body y-axis (ft/s)
w_b	Helicopter body velocity along body z-axis (ft/s)
X	Inertial position in inertial x-axis (ft)
Y	Inertial position in inertial y-axis (ft)
Z	Inertial position in inertial z-axis (ft)
Δ	Discrete step (time)
δ_a	Lateral cyclic input (percent)
δ_b	Longitudinal cyclic input (percent)
δ_c	Collective input (percent)
δ_p	Pedal input (percent)

Presented at 44th European Rotorcraft Forum, Delft, The Netherlands, 19-20 September, 2018

ϕ Roll attitude (rad)

θ Pitch attitude (rad)

ψ Yaw attitude (rad)

σ Standard deviation

τ Time constant (s)

Subscripts

f Final (time)

h Physical quantity associated with the helicopter/vehicle

i Trajectory or random control element number

j Current time instant

ref Reference

s Physical quantity associated with the ship

T Terminal

win Window

0 Initial (time)

2. INTRODUCTION

Rotorcraft shipboard landing is one of the most challenging and training intensive helicopter operations. In order to ensure a smooth touch down, pilot must continuously observe the ship motion while adjusting control inputs. Helicopter shipboard landing operations involve significant caution in order to account for random deck motions, turbulence effects due to airflow through the ship's superstructure, and degraded visual environments due to weather conditions and time of the day. Furthermore, during shipboard landing operations, vehicle limits in terms of power margin, control authority, attitude constraints, etc., may be encountered while trying to maintain zero relative velocity with the ship deck. This could lead to pilot fatigue and extended task time since the pilot typically waits for a quiescent period to land on the ship deck.

Multiple studies have been carried out to develop controllers which involve ship deck motion prediction algorithms and ship air wake turbulence models. References 1 through 4 have performed non-real-time simulations of shipboard operations with workload estimated using pilot models. Vision-based control has been tested in Refs. 5 through 8. Flight controllers for ship approach and landing have been presented in Refs. 9 and 10. Another suitable strategy has been to provide trajectory guidance to the pilot during the task. Ref. 11 presents objective functions for optimal path guidance for shipboard landing.

Model predictive control (MPC) methods have been a promising solution to provide pilot assist function, but with limited success. The caveat is their dependence on explicit optimization. Since the inclusion of ship deck motions and air wake effects make the problem stochastic, this limits the capability of MPC methods to provide a computationally efficient solution for real time application unless solution fidelity is compromised.

Model Predictive Path Integral (MPPI) approach (Ref. 12) is based on stochastic optimal control framework and provides solutions through implicit optimization. It leverages the parallelization technique in computation, thus making it a suitable computational scheme for real time guidance.

A preliminary study on the application of MPPI approach to rotorcraft shipboard landing task has been carried out in Ref. 13. The current paper is an extension of the study conducted in Ref. 13. The focus of the paper is to understand the impact of incorporating yaw attitude constraint in the objective function of the optimization problem. Since the overarching goal of this work involves real time guidance, a high-fidelity nonlinear model has been introduced to represent the actual vehicle while a linear 6-DOF model is used to predict vehicle behavior. Lastly, a brief sensitivity analysis has been done to understand the effect of the prediction horizon on the vehicle response and terminal errors.

3. MPPI METHOD FOR TRAJECTORY OPTIMIZATION

3.1. Method Summary

Reference 13 provides a detailed overview of the methodology of MPPI as applied to the shipboard landing task. To summarize, the MPPI approach evaluates an appropriate control based on a chosen performance measure using an onboard model of the vehicle dynamics for response prediction. Several sample control vectors are constructed as random perturbations about an initial estimate.

(1) $$u_i = u_m + du_i, \quad i = 1 \; to \; M$$

A chosen performance index is evaluated for each sample trajectory resulting from the sample control vectors. The updated control vector is obtained as shown below (Eq. 2).

Presented at 44th European Rotorcraft Forum, Delft, The Netherlands, 19-20 September, 2018

(2) $u_p = u_m + \frac{1}{M}\sum_{i=1}^{M}(du_i)e^{-J_i}$

The exponential weighting allows the control update to be heavily biased towards trajectories with lower cost values and implicitly forces the control vector towards the optimal solution.

Table 1. DDG-51 Combatant ship representative motion statistics, heave as dominant motion.

		Sea State		
		Low	Medium	High
Horizontal Velocity (ft/sec)	RMS	0.18	0.36	0.73
	Mean	8.1	33.5	50.0
	Max/ Min	8.8/ 7.5	34.5/32.0	51.7/ 46.1
Lateral Velocity (ft/sec)	RMS	0.74	0.89	1.76
	Mean	0.0	0.0	0.0
	Max/ Min	2.5/ -2.1	3.2/-3.4	6.3/ -5.6
Vertical Acceleration (ft/sec^2)	RMS	1.14	2.43	5.13
	Mean	0.0	0.0	0.0
	Max/ Min	3.5/ -4.2	8.3/-8.6	16.8/ -19.2

3.2. Ship deck Motion Model

The ship motion model used in this study is representative of a destroyer type ship such as the DDG-51. The US Navy Office of Naval Research (ONR), Naval Surface Warfare Center Carderock Division (NSWCCD) provided the statistical data required to generate the ship motion in the x-, y- and z-axes. Ship motion in the z-axis (heave motion) is generated from random acceleration with mean and standard deviation of the selected sea state for the DDG-51 ship. The ship's forward velocity is maintained at 19.8 knots (33.5 ft/s) for all the sea states. Surge and sway motions are randomly generated with the standard deviation for the selected sea state. The representation is shown in Table 1. In comparison to Ref. 13, the ship's forward velocity is kept at a constant for all sea states for the current study.

3.3. MPPI using a Linear Helicopter Model

Reference 13 presented the results for a proof-of-concept study using MPPI approach for trajectory guidance in shipboard landing using a linear helicopter model as the prediction model as well as the truth model. The performance measure chosen was a quadratic penalty function which included cost terms for penalizing deviations in following a reference trajectory and for minimizing control effort. The study also presented the results for two cases of optimization – shrinking horizon method and receding horizon method, where the former involves vehicle response prediction from current time instant t_i up to the final time t_f, while the latter involves vehicle response prediction from the current time instant t_i up to a chosen time window into the future $t_i + t_{win}$. The discrete time step for the simulations was $\Delta t = 0.1$ s.

3.3.1. Introduction of Yaw Attitude Constraint

The proof-of-concept study conducted in Ref. 13, without any yaw attitude constraints in the performance index, resulted in large terminal errors in the yaw attitude. The current study attempts to rectify the same by introducing a yaw constraint in the performance measure to observe the effect on the overall performance. This paper will focus on results from the receding horizon optimization method alone. This is because the shrinking horizon method is satisfactory only as long as the prediction from onboard model is accurate and is similar to the truth model. However, for actual application, the truth model would be the actual helicopter which would be different from the onboard model. Hence, by adopting the receding horizon method, the loss of fidelity and increased computational cost can be avoided. The details of the receding horizon method for optimization has been presented in Ref. 13. For this study, the prediction window has been set to $t_{win} = 2$ sec.

Using a linear helicopter model as a representation of the vehicle, two cases of ship landing are considered – A) without any lateral offset, i.e. the helicopter is lined up with the course of the ship, and B) with lateral offset, where the helicopter approaches the ship from the port side. The landing is completed with a fixed time of 40 seconds for both cases. A sketch of Case A landing is shown in Fig. 1. The landing phase considered in this part of the study is as follows: At the start time (t_0), the

Presented at 44th European Rotorcraft Forum, Delft, The Netherlands, 19-20 September, 2018

vehicle is in level flight with a speed of 40 knots (67.5 ft/s) and its location at 100 ft above and 1100 ft behind the ship deck. The ship is moving at a constant speed of 19.8 knots (33.5 ft/s). The total landing time (t_f-t_0) is 40 s. Figure 2 shows the sketch of Case B landing. In this case, the vehicle begins landing from the port side of the ship with a 550 ft lateral offset.

The truth model and the onboard model for prediction are the same linearized model of the UH-60 helicopter obtained from FLIGHTLAB®, a high-fidelity industry-standard tool for rotorcraft flight dynamics modelling and analysis (Ref. 14). The vehicle is trimmed in forward flight at 40 knots (67.5 ft/s) airspeed and the corresponding linear model obtained is of the form

(3) $$\dot{x} = Ax + Bu$$

where x is the vector of helicopter states (body axes) and u is the control inputs vector.

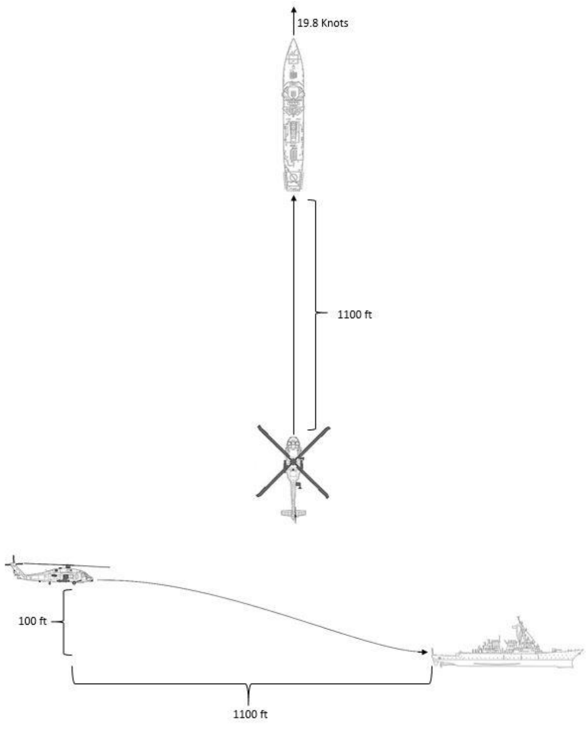

Figure 1. Symmetric landing phase (zero lateral offset) [13].

Since the MPPI approach requires an initial control profile, the initial estimate for this study is obtained from optimal control theory. The performance measure is similar to the earlier study with an additional reference yaw angle trajectory (Eq. 4).

(4) $$J = \frac{1}{2}\int_{t_0}^{t_f}[(z - Cx)^T Q(z - Cx) + u^T Ru]dt$$

where x and u represent the states and control inputs of the model. z represents the reference trajectory (position, velocity and yaw angle) to be followed in the inertial coordinates and C represents the matrix for obtaining the corresponding inertial quantities from the state vector x. Q is the weighting matrix for error between the desired and actual vehicle response and R is the weighting matrix for control effort. For this trajectory following problem, the control law is based on linear state feedback to follow a desired output as elaborated in Ref. 15.

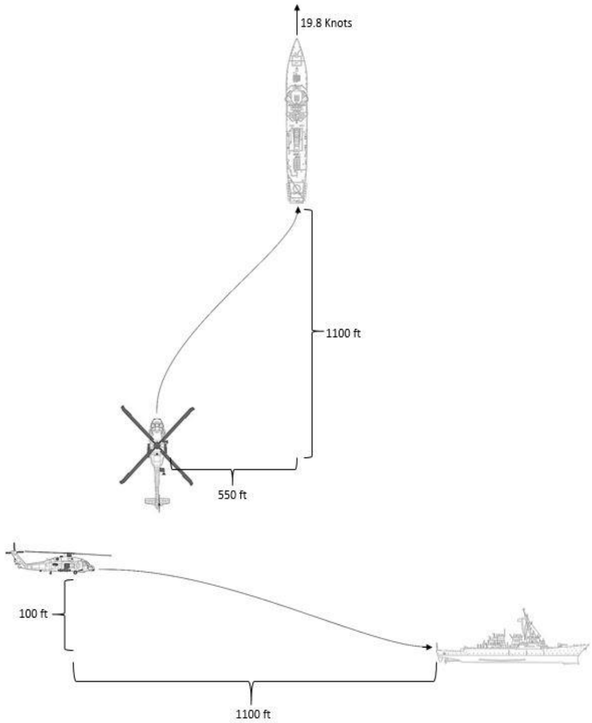

Figure 2. Landing phase with lateral offset [13].

The reference trajectories are generated using a point mass vehicle represented in the form of a first order acceleration model (Eq. 5) from solving the boundary value problem for a fixed terminal ship deck by minimizing vehicle accelerations.

(5) $$\begin{bmatrix}\dot{z}\\ \dot{w}\\ \dot{a}\end{bmatrix} = \begin{bmatrix}0 & 1 & 0\\ 0 & 0 & 1\\ 0 & 0 & -\frac{1}{\tau}\end{bmatrix}\begin{bmatrix}z\\ w\\ a\end{bmatrix} + \begin{bmatrix}0\\ 0\\ \frac{a_c}{\tau}\end{bmatrix}$$

This model represents the dynamics along the vertical axis alone, where τ (set to 1*s* in this study) is the time constant of an assumed trajectory controller with command acceleration as input. Similar models are used for representing motion along the remaining longitudinal and lateral axes. For the yaw angle reference trajectory, the reference velocity trajectories were used to determine the yawing required for zero sideslip,

Presented at 44th European Rotorcraft Forum, Delft, The Netherlands, 19-20 September, 2018

particularly for the lateral offset approach. Thus, the reference trajectories (generated independently for all the axes) for inertial positions and velocities, and yaw angle are obtained and used to calculate the optimal control profile which serves as the initial value for the control vector required in the MPPI approach.

With an initial estimate for the control vector in MPPI thus obtained, the same performance measure as shown in Eq. 4 augmented with terminal cost terms (see Eqs. 6 and 7) is selected for arriving at the helicopter controls during landing, using the optimal trajectories obtained with the point mass model as reference. Note that the terminal cost term shown in Eq. 8 includes the random deck motions (heave, surge and sway). The number of random control vectors or trajectories is maintained at M = 100 with a time step of $\Delta t = 0.1$ s. The random control perturbations are kept at 10% for the longitudinal controls and at 1% for the lateral controls. This was done to ensure lower lateral errors. Since the linear model is coupled in the X, Y, and Z axes, the entire MPPI evaluation is done together for all degrees of freedom. Trajectories which yielded terminal position and velocity errors more than 5 ft and 3 ft/s in all three axes, and terminal yaw angle errors more than 5 degrees simultaneously were rejected. Note that this specific rejection criterion used, where trajectories with terminal errors outside the selected bounds in one or two axes would be allowed, could result in a degraded MPPI solution. This aspect on how to devise a more robust rejection criterion will be addressed in the future.

The truth as well as onboard models have the state and control vectors

$$x = [X \quad Y \quad Z \quad \varphi \quad \theta \quad \psi \quad u_b \quad v_b \quad w_b \quad p \quad q \quad r]^T$$

and $u = [\delta_b \quad \delta_a \quad \delta_p \quad \delta_c]^T$ respectively, with the reference trajectory vector as

$$z = [U_{ref} \quad V_{ref} \quad W_{ref} \quad X_{ref} \quad Y_{ref} \quad Z_{ref} \quad \psi_{ref}]^T$$

The performance measure tested for MPPI approach in the receding horizon optimization method is

$$J_i = \frac{1}{2}\int_{t_j}^{t_j + t_{win}} [(z - Cx)^T Q (z - Cx) + u^T R u] dt, \qquad when\ t_j + t_{win} < t_f \tag{6}$$

$$J_i = \frac{1}{2}\int_{t_j}^{t_f} [(z - Cx)^T Q (z - Cx) + u^T R u] dt + F\left[\left(Cx(t_f) - z_s(t_f)\right)^T Q_T \left(Cx(t_f) - z_s(t_f)\right)\right], \quad when\ t_j + t_{win} = t_f \tag{7}$$

where

$$z_s = [U_s \quad V_s \quad W_s \quad X_s \quad Y_s \quad Z_s \quad 0]^T$$

z_s represents the ship deck positions, velocities and yaw angle considering random deck motion and Q_T represents the terminal error weighting matrix. *F,* mentioned in Eq. 7, is a time dependent weighting function, logarithmically spaced from $10^{0.3}$ to $10^{0.5}$, to trade between path cost and terminal cost in the solution. This function favors terminal constraints rather than path cost as the vehicle approaches the ship deck. In Eq. 7, the first term represents the path cost while the second term represents the terminal cost. The terminal cost contains the sum of the square of the error between the reference and actual positions and velocities in all axes, and the square of the error between the desired terminal yaw attitude, which is the same as the ship yaw angle (0 deg in this study), and the actual helicopter yaw attitude.

3.3.2. Results for Zero Lateral Offset Approach (Case A Landing)

For the symmetric approach landing, the reference trajectories for X and Z inertial axes are generated using the same point-mass model represented as a first order command acceleration model independently, while the reference trajectories for Y axis and yaw angle are maintained at zero.

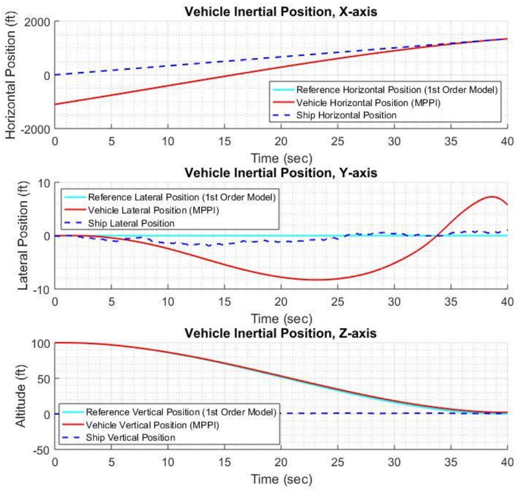

Figure 3. Vehicle positions (MPPI) and ship deck positions with reference trajectories in the X, Y, Z-axes for zero lateral offset (receding horizon) [6-DOF helicopter linear model].

Figures 3 through 6 portray the results for the linear helicopter model for zero lateral offset ship landing approach in medium sea state with receding horizon optimization method. The vehicle begins the landing phase from a height of 100 ft above and

Presented at 44th European Rotorcraft Forum, Delft, The Netherlands, 19-20 September, 2018

1100 ft behind the ship deck with a velocity of 67.5 ft/s. It is observed that the MPPI results closely match with the reference trajectories in the X and Z axes. Although there are deviations in following the Y position reference trajectory, the terminal position error is around 5 ft and nearly 0 ft/s in terminal velocity error.

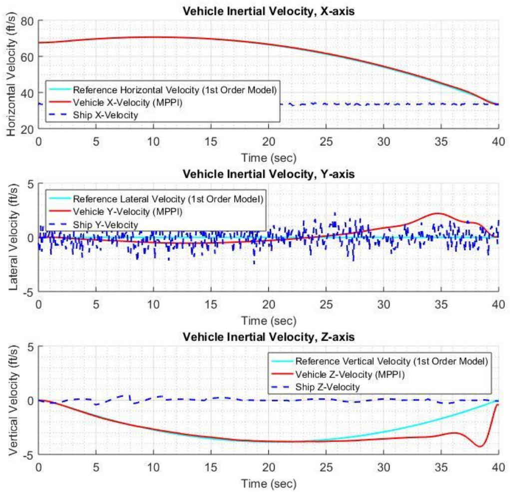

Figure 4. Vehicle velocities (MPPI) and ship deck velocities with reference trajectories in the X, Y, Z-axes for zero lateral offset (receding horizon) [6-DOF helicopter linear model].

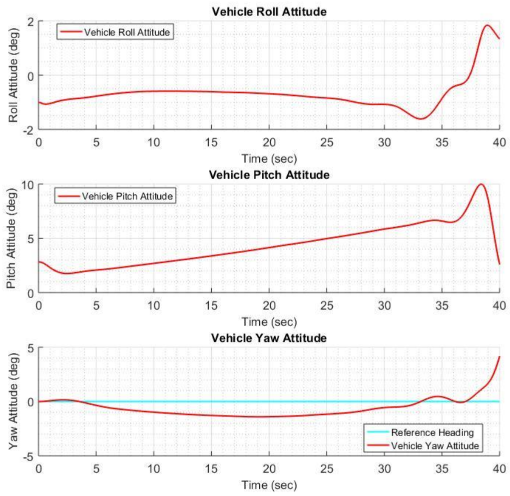

Figure 5. Vehicle attitude (MPPI) with reference yaw angle trajectory for zero lateral offset (receding horizon) [6-DOF helicopter linear model].

Figure 5 indicates a sharp pitch attitude change towards the end of the landing. This is because the reference trajectory is generated for a point mass vehicle represented as a first-order command acceleration model, which does not have any attitude considerations while minimizing accelerations. Hence, the generated trajectories in positions have a near constant slope except towards the end where there is a distinct curve, which causes a sharp pitch up in order to maintain the reference position and velocity profiles. As a result, the vertical velocity is also affected due to its dependence on pitch attitude (Fig. 4). No constraints are placed on attitude but the maximum pitch attitude stays within an acceptable limit of 15 degrees. Furthermore, the roll attitude changes by a maximum of 2 degrees from the trim value at the terminal time. The yaw angle shows a maximum change of 2 degrees during the landing phase and lands with a terminal error of 4 degrees, which is within the desired limit. Unlike the results in Ref. 13, the oscillations in roll and yaw angles throughout the landing phase are reduced due to the introduction of the yaw attitude cost term. On the contrary, the deviations from the Y position reference trajectory are higher. The control input changes are significant in the longitudinal cyclic and collective, compared to the lateral cyclic and pedal (Fig. 6).

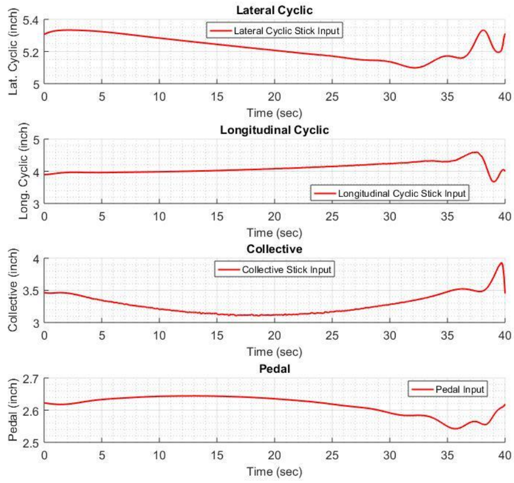

Figure 6. Vehicle controls (MPPI) during landing for zero lateral offset (receding horizon) [6-DOF helicopter linear model].

Table 2 summarizes the results for zero lateral offset ship landing for the 6-DOF helicopter linear model averaged over 20 simulations in each sea state. The average number of usable trajectories remains at 99.75 (out of 100) with an average running time per simulation of 7.07 s.

The velocity terminal errors are within the limit of 3 ft/s in all axes for all sea states. While the position terminal errors are within 5 ft for X and Z axes, the Y axis has slightly larger errors. This is because with emphasis now placed on vehicle yaw attitude as an additional constraint, the error in the lateral axis increases a little. Also, the specific rejection criterion used in this study, where those trajectories with terminal errors outside the selected bounds simultaneously in all three axes and yaw angle alone were rejected, could lead to degraded MPPI solutions. This is evident from the Y axis terminal errors for all sea states. The terminal yaw attitude error remains within the limit of 5 degrees in all sea states.

Table 2. X, Y and Z axes terminal position and velocity errors, and terminal yaw angle error averaged over 20 simulations for complete linear helicopter model with moving ship deck and zero lateral offset (receding horizon) [6-DOF helicopter linear model].

		Sea State		
		Low	Medium	High
X-Axis	Final Position Error (ft)	1.64	1.47	1.93
X-Axis	Final Velocity Error (ft/s)	0.24	0.48	0.35
Y-Axis	Final Position Error (ft)	5.93	6.23	6.09
Y-Axis	Final Velocity Error (ft/s)	0.51	0.55	1.29
Z-Axis	Final Position Error (ft)	2.15	1.70	2.48
Z-Axis	Final Velocity Error (ft/s)	0.52	0.43	0.47
Yaw	Final Angle Error (deg)	4.16	4.14	4.15

3.3.3. Results for Lateral Offset Approach (Case B Landing)

This subsection presents the sample results with the linear model of the helicopter for ship landing with a lateral offset. The reference trajectories for X, Y and Z axes are generated independently using the first order acceleration model as described by Eq. 5. The reference trajectory for the yaw angle was generated using the reference velocity trajectories to determine change in yaw that is desired to maintain zero sideslip. The helicopter starts at 1100 ft behind, 100 ft above and 550 ft to the left of the ship in the inertial frame and completes the landing in 40 seconds (see Fig. 2).

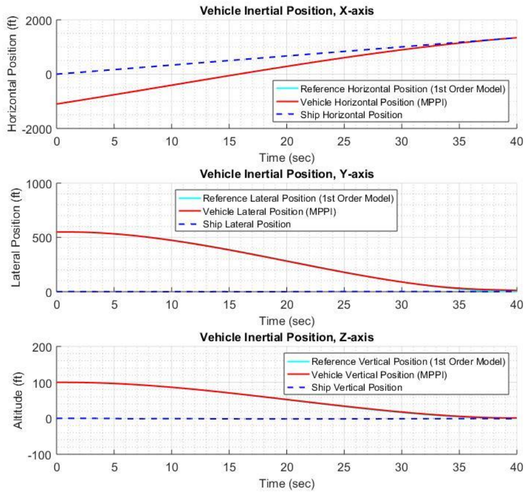

Figure 7. Vehicle positions (MPPI) and ship deck positions with reference trajectories in the X, Y, Z-axes for lateral offset (receding horizon) [6-DOF helicopter linear model].

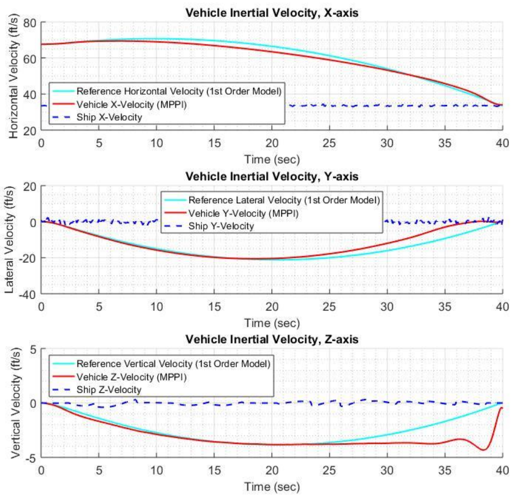

Figure 8. Vehicle velocities (MPPI) and ship deck velocities with reference trajectories in the X, Y, Z-axes for lateral offset (receding horizon) [6-DOF helicopter linear model].

Figures 7 through 10 present the results for lateral offset approach in medium sea state with random

Presented at 44th European Rotorcraft Forum, Delft, The Netherlands, 19-20 September, 2018

deck motion. The representative results show that the position and velocity trajectories are followed closely throughout. In terms of attitude, the roll angle shows a peak change of 5 degrees but the terminal value is close to 0 degrees. The pitch angle shows a sharp change towards the end which was observed for the symmetric approach as well. The yaw angle follows the reference well with an error of 2 degrees or lower throughout except close to the terminal time where the error is around 6 degrees. The controls show a significant change in lateral cyclic compared to the symmetric approach case owing to the changes in the lateral axis.

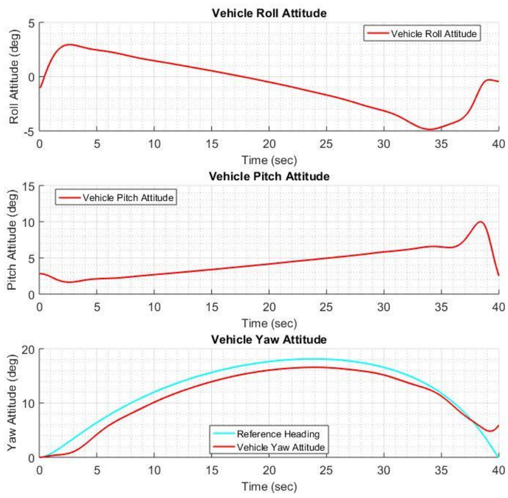

Figure 9. Vehicle attitude (MPPI) with reference trajectory in yaw angle for lateral offset (receding horizon) [6-DOF helicopter linear model].

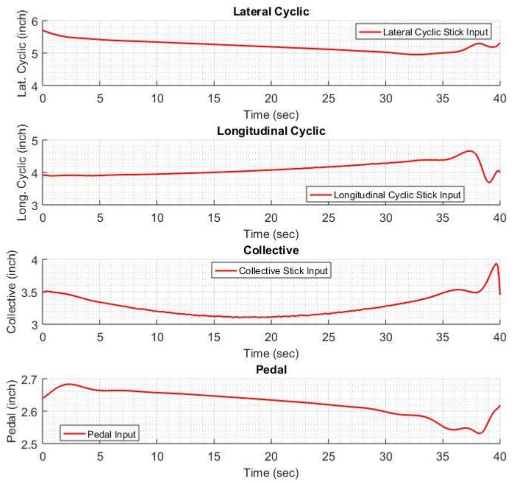

Figure 10. Vehicle controls (MPPI) during landing for lateral offset (receding horizon) [6-DOF helicopter linear model].

Table 3 presents the results for all sea states, each averaged over 20 simulations. Similar to the symmetric approach, the Y axis terminal position errors are higher compared to the X and Z axes. Furthermore, the terminal yaw attitude error is also higher than the symmetric approach case. The specific trajectory rejection criterion allows degradable solutions which would allow cases where even one or two constraints are violated. Additionally, since the receding horizon method only allows prediction to a limited time into the future, it is not possible to predict and correct these terminal errors until the vehicle is close to the ship deck.

Table 3. X, Y and Z axes terminal position and velocity errors, and terminal yaw angle error averaged over 20 simulations for linear helicopter model with moving ship deck and lateral offset (receding horizon) [6-DOF helicopter linear model].

		Sea State		
		Low	**Medium**	**High**
X-Axis	Final Position Error (ft)	1.69	2.12	2.39
	Final Velocity Error (ft/s)	0.60	0.68	0.64
Y-Axis	Final Position Error (ft)	9.19	8.56	7.96
	Final Velocity Error (ft/s)	0.40	0.62	1.14
Z-Axis	Final Position Error (ft)	0.99	0.81	2.66
	Final Velocity Error (ft/s)	0.56	0.44	0.53
Yaw	Final Angle Error (deg)	5.98	5.95	5.97

3.4. MPPI using a Nonlinear Helicopter Model

The previous studies investigated the outcome when the prediction model. i.e., model used in MPPI solution, and the truth model are linear and identical. However, in real application, the truth model will be an actual helicopter and with the

Presented at 44th European Rotorcraft Forum, Delft, The Netherlands, 19-20 September, 2018

objective of developing a real time guidance solution to the shipboard landing problem, it is important to consider a truth model in simulation which gives a response similar to the actual helicopter. Thus, the linear truth model, which was implemented earlier, has now been replaced with a high fidelity nonlinear model.

FLIGHTLAB®, an industry-standard tool for rotorcraft flight dynamics modelling and analysis (Ref. 14), applies a multi-body dynamics formulation that combines blade element based unsteady aerodynamics modelling for a high-fidelity flight dynamics simulation. It allows the user to select a baseline model and modify the parameters and perform simulations depending on the study of interest. For the current study, a rotorcraft model with an articulated rotor with rigid blades, 3-state inflow, and quasi-steady airloads has been chosen. This model, with its configuration similar to the UH60, is trimmed at 40 knots forward flight and used in this study. The communication between FLIGHTLAB and the MPPI algorithm was established using an SDX-MEX function. This function enabled the transfer of the vector of control inputs at each time instant to the FLIGHTLAB nonlinear model, wait for the nonlinear response for the discrete time step of 0.1 second and then receive the 6-DOF rigid body states, which now represent the truth model response for that time instant. A linear model of the helicopter was retained as the MPPI prediction model.

During the landing phase, the helicopter begins at 40 knots (67.5 ft/s) and within 40 seconds, reaches the ship which is moving at 19.8 knots (33.5 ft/s). The linear model extracted from FLIGHTLAB, linearized about 40 knots, was used as the MPPI prediction model. It is important to note that for the studies using a nonlinear truth model, the same performance measure which was used for the linear truth model case has been tested to ensure consistency. The results presented in the following subsection were obtained using the receding horizon optimization method (where t_{win} = 2 seconds) for the symmetric landing approach in medium sea state. It is critical to mention that the nonlinear truth model response (6DOF states) at every instant is used to reinitialize the MPPI model states for prediction during the simulation. This would ensure basic correction in the prediction model, which would otherwise result in significant errors. Furthermore, the simulation was simplified by not incorporating the random ship deck motion model in order to understand the outcome of using different prediction and truth models. This means that the ship is moving at a constant speed of 19.8 knots (33.5 ft/s) in the forward direction (along inertial X axis), with no surge, sway or heave motions.

3.4.1. Results with a Nonlinear Truth Model

This subsection presents the representative and tabulated results when a single linear model, linearized about 40 knots, is used as the MPPI prediction model.

Figures 11 through 14 show the representative results for a moving ship without random deck motion where the responses shown are the nonlinear truth model when a linear prediction model is used in MPPI. From Figs. 11 and 12, it is observed that the lateral errors are the most significant, followed by the vertical motion errors. This is expected as the current linear model used for prediction loses its fidelity as the vehicle moves away from the trim state of 40 knots about which the model is extracted from the nonlinear model. On comparing Figs. 4 and 12, it is visible that while the linear truth model follows the reference velocity trajectories in Y and Z axes, the nonlinear model shows significant deviations for the same performance measure. As a result, this difference gets integrated over time resulting in large terminal position errors for the nonlinear truth model case unlike the linear truth model case. This can be verified from comparing Tables 2 and 4.

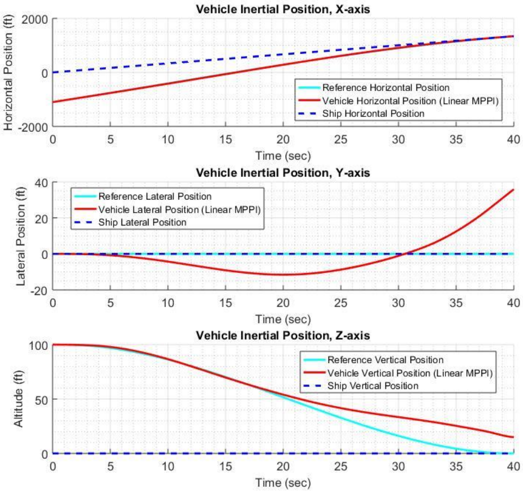

Figure 11. Nonlinear truth model inertial positions for a linear MPPI model without random deck motion in symmetric landing case.

Although the roll and pitch attitude changes are within limits, the yaw angle changes by 12 degrees towards the terminal time as seen in Fig. 13. Furthermore, the change in pitch attitude is not as sharp as the linear model case.

Presented at 44th European Rotorcraft Forum, Delft, The Netherlands, 19-20 September, 2018

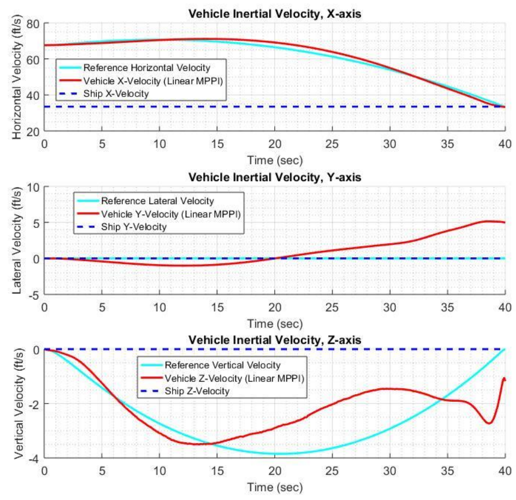

Figure 12. Nonlinear truth model inertial velocities for a linear MPPI model without random deck motion in symmetric landing case.

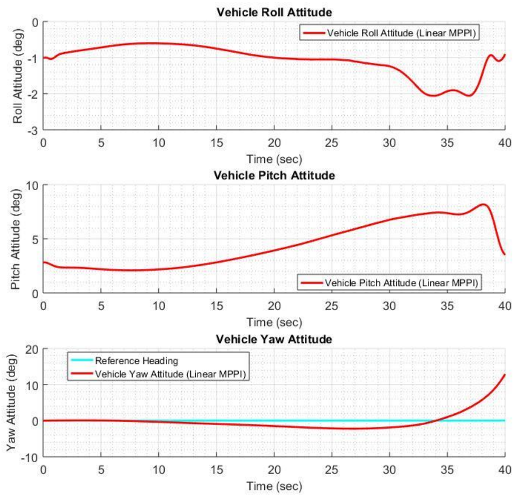

Figure 13. Nonlinear truth model attitude for a linear MPPI model without random deck motion in symmetric landing case.

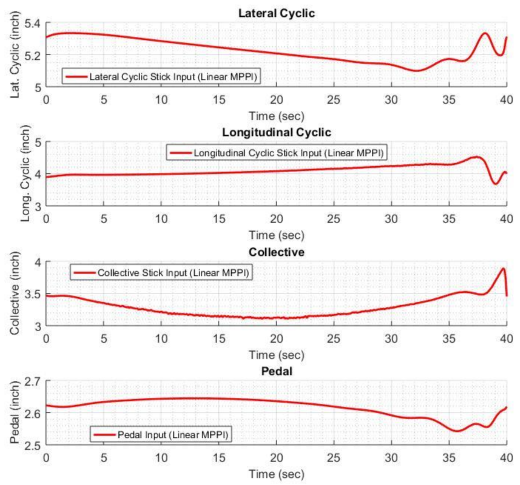

Figure 14. Control inputs to the nonlinear truth model with a linear MPPI model without random deck motion in symmetric landing case.

Table 4 shows the terminal errors in the nonlinear truth model response and corresponding performance cost when a linear model is used in MPPI averaged over 10 simulations. It is observed that the terminal errors are within the limits for the horizontal position and velocity as well as the vertical velocity. The lateral position error is the most significant followed by the vertical position error. This can be attributed to the inability of a single linear model to accurately predict the response of a nonlinear model for a given sequence of control inputs. This could be rectified by incorporating a scheduled linear model or linear stitched model for the MPPI prediction. Furthermore, since the horizontal errors are still within the limits for the current scenario, the specific trajectory rejection criterion of discarding only those trajectories which yield large errors in all axes simultaneously, leads to degraded MPPI solutions with large lateral and vertical errors.

Table 4. X, Y and Z axes terminal position and velocity errors, terminal yaw angle error and performance cost averaged over 10 simulations for nonlinear truth model and linear MPPI model.

Terminal Position Errors (ft)			**Terminal Velocity Errors (ft/s)**			**Term. Yaw Angle Error (deg)**	**Performance Cost**				
X	**Y**	**Z**	**U**	**V**	**W**		**Path**	**Term. X**	**Term. Y**	**Term. Z**	**Psi**
1.53	34.26	14.78	0.36	4.88	1.17	13.23	351.6	9.97	3791	695.4	0.17

Presented at 44th European Rotorcraft Forum, Delft, The Netherlands, 19-20 September, 2018

3.4.2. Sensitivity Analysis with t_{win}

One of the key parameters of the receding horizon method of optimization is the window or horizon of prediction. It is important to understand how the extent of future prediction could affect the performance of the MPPI method, in terms of the terminal errors and performance cost. This subsection focuses on analysing the impact of changing window of prediction associated with the MPPI model when a linear model is used for prediction. The truth model is retained as the FLIGHTLAB nonlinear model for this sensitivity analysis. As mentioned previously, the symmetric approach case is studied without random deck motion. For this sensitivity analysis, t_{win} = 1, 2, 3 and 5 seconds were considered.

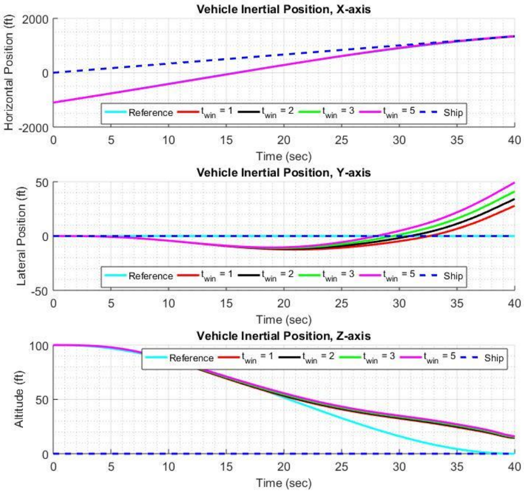

Figure 15. Nonlinear truth model inertial positions for a linear MPPI model without random deck motion in symmetric landing case for varying values of t_{win}.

Figures 15 through 18 show the effect of varying t_{win} when a linear model is used for prediction and the nonlinear model represents the truth model. Figures 15 and 16 show that as t_{win} is increased, the terminal errors also increase. This is because the linear model does not accurately predict the nonlinear model response and by increasing the horizon of prediction, it results in the growth of error, which subsequently affects the control update. However, the terminal error in yaw angle decreases as t_{win} increases (Fig. 17). This could be attributed to the increased duration where the terminal yaw constraint remains active (towards the last 1, 2, 3 or 5 seconds) due to increasing prediction window. This opposing trend is possibly due to the response of the linear prediction model, i.e. the terminal error as predicted using a linear model could be dominated by the error in yaw attitude compared to the position and velocity errors, which could eventually lead to a solution with decreasing yaw angle error but increasing position and velocity errors at the terminal time. This trend can be further verified using the results in Table 5.

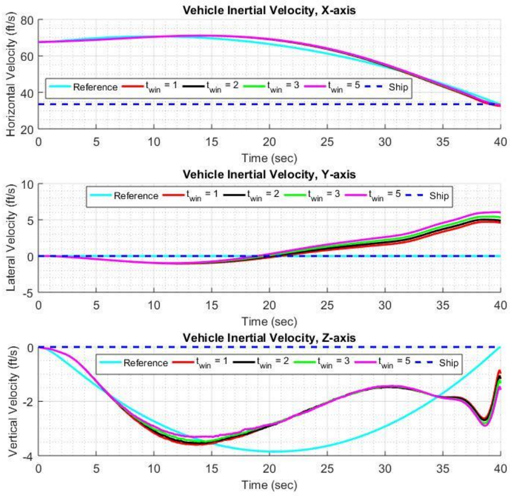

Figure 16. Nonlinear truth model inertial velocities for a linear MPPI model without random deck motion in symmetric landing case for varying values of t_{win}.

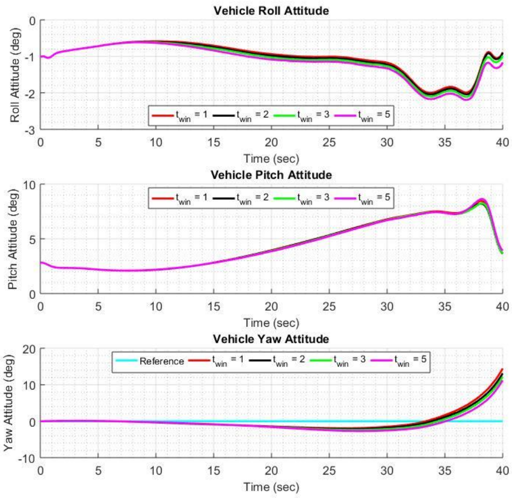

Figure 17. Nonlinear truth model attitude for a linear MPPI model without random deck motion in symmetric landing case for varying values of t_{win}.

Presented at 44th European Rotorcraft Forum, Delft, The Netherlands, 19-20 September, 2018

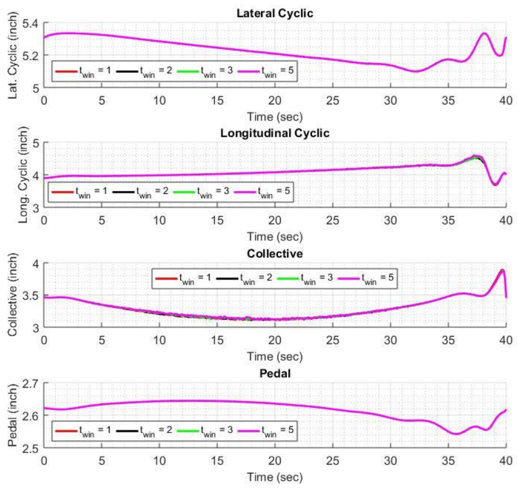

Figure 18. Control inputs to the nonlinear truth model using a linear MPPI model without random deck motion in symmetric landing case for varying values of t_{win}.

Table 5 shows the comprehensive results for varying t_{win} averaged over 10 simulations for a linear MPPI model. A common observation is that as t_{win} increases, the terminal X position error also increases, i.e. the helicopter begins landing behind the ship on average when t_{win} = 1 sec and by the time t_{win} is increased to 5 seconds, the helicopter lands well ahead of the ship. This indicates that as the window of prediction increases, the error grows due to the differences between the prediction model and the truth model. Similarly, the terminal Y and Z position errors also increase due to the same reason.

Furthermore, the terminal velocity error in Y and Z axes increase in a similar manner. Additionally, the yaw angle terminal error decreases as t_{win} increases. As explained earlier, the opposing trend is possibly due to the prediction model being different from the truth model, which could yield larger terminal yaw angle errors compared to position and velocity errors, thereby causing the solution to be driven by the terminal yaw attitude error more. The path cost also uniformly increases indicating the increasing error in following the reference trajectory and control effort. The computational time increases with the prediction window as expected. The average number of usable trajectories remains 99.75 for all t_{win} due to the nature of the specific trajectory rejection criterion. Thus, when the prediction model is different from the truth model, it is better to use a shorter horizon for prediction to minimize error accumulation and to reduce the computational time.

Table 5. X, Y and Z axes terminal position and velocity errors, terminal yaw angle error and path cost averaged over 10 simulations for nonlinear truth model and linear MPPI model with varying t_{win}.

		Terminal Position Errors (ft)			Terminal Velocity Errors (ft/s)			Terminal Yaw Angle Errors (deg)	Path Cost	Avg. No. of Usable Trajs.	Running Time (s)
		X	Y	Z	U	V	W	Psi			
Prediction Window t_{win} (seconds)	1	-2.73	28.15	14.52	-0.99	4.60	-0.97	14.35	331.58	99.75	10.09
	2	1.71	34.14	14.81	-0.35	4.87	-1.17	13.19	351.11	99.75	11.68
	3	5.32	39.38	15.18	0.08	5.18	-1.33	12.26	371.82	99.75	13.29
	5	9.35	49.75	15.87	0.08	5.91	-1.70	11.01	418.51	99.75	16.25

Presented at 44th European Rotorcraft Forum, Delft, The Netherlands, 19-20 September, 2018

4. CONCLUDING REMARKS

The paper, as an extension to previous work, investigates the impact of introducing yaw constraint in the performance measure. Since the receding horizon method for optimization is more realistic owing to the differences which will exist between the prediction and truth models in actual application, this method has been adopted throughout the work. First, a study is conducted to assess the new performance index by considering a linearized 6-DOF helicopter model as the prediction as well as truth models. The next subsection focused on using a nonlinear model as the truth model for better representation of the actual vehicle and considered a single linear prediction model which is linearized about the same flight speed as the nonlinear model is trimmed. The last section focused on studying the impact of increasing the window of prediction on the terminal errors and the path cost of the nonlinear truth model.

The results of this study show that by introducing a yaw attitude reference and terminal constraint, it is possible to restrict the yawing motion of the helicopter and ensure a reasonable terminal yaw angle. However, this leads to an increase in the lateral position error and it is important to maintain a balance between the two quantities. The study also shows that the single linear model as used in the current form is unable to predict the nonlinear model response well, resulting in increased terminal errors. This prediction model inaccuracy could perhaps be rectified by developing an appropriate linear stitched model for improved MPPI performance. Alternately, an adaptive model that can capture the model uncertainty in the linear model would also improve the MPPI performance. It is also possible that tweaking of the weighting values in the performance measure can lead to improved MPPI performance. Furthermore, the specific rejection criterion in stochastic averaging of sample trajectories, where the sample trajectories with terminal errors outside the selected bounds in all axes simultaneously alone were rejected, led to degraded MPPI solutions. Although the linear model used for prediction was not capable of reducing terminal errors in the nonlinear model response, it allowed a brief study on the sensitivity of the window of prediction to be conducted. This study showed that increasing the prediction horizon leads to increased terminal position errors but decreasing terminal yaw attitude errors. However, the increasing path cost and computational time additionally suggest that a smaller window of prediction yields better MPPI performance.

Future study will consider ship air wake effects by introducing representative air wake models. A more suitable linear stitched prediction model will be used for improved accuracy and the random ship deck motions that include pitching and rolling motions, in addition to the existing heave, surge and sway motions, will be incorporated. Parallelization of the algorithm for better time efficiency and real-time application will be established. This step would allow the number of sample trajectories to be increased without sacrificing computational time and help explore the aspect of devising a more robust criterion for rejecting sample trajectories that yield terminal errors outside the desired bounds. Additionally, future work will include piloted simulation evaluations of shipboard landings with MPPI trajectory optimization and guidance.

5. ACKNOWLEDGMENTS

This study is supported under the NRTC Vertical Lift Rotorcraft Center of Excellence (VLRCOE) from the U.S. Army Aviation and Missile Research, Development and Engineering Center (AMRDEC) under Technology Investment Agreement W911W6-17-2-0002, entitled Georgia Tech Vertical Lift Research Center of Excellence (GT-VLRCOE) with Mahendra Bhagwat as the Program Manager. The authors would like to acknowledge that this research and development was accomplished with the support and guidance of the NRTC. The authors would also like to thank the team and staff at Advanced Rotorcraft Technology, Inc., for FLIGHTLAB support. The authors would like to acknowledge Robert Walters for his assistance and the discussions pertaining to this project. The views and conclusions contained in this document are those of the authors and should not be interpreted as representing the official policies, either expressed or implied, of the AMRDEC or the U.S. Government. The U.S. Government is authorized to reproduce and distribute reprints for Government purposes notwithstanding any copyright notation thereon.

6. REFERENCES

[1]Bradley, R. and Turner, G. "Simulation of the human pilot applied at the helicopter/ship dynamic interface," American Helicopter Society 55th Annual Forum, Montreal, Canada, May 1999.

[2]Turner, G., Brindley, G. and Bradley, R. "Simulation of pilot control activity for the prediction of workload ratings in helicopter/ship operations," 26th European Rotorcraft Forum, The Hague, Netherlands, September 2000.

[3]Hess, R.A., "A Simplified Technique for Modeling Piloted Rotorcraft Operations Near Ships," AIAA Atmospheric Flight Mechanics Conference and Exhibit, San Francisco, California, Aug. 15-18, 2005. AIAA-2005-6030.

[4]Lee, D. and Horn, J.F., "Simulation of Pilot Workload for a Helicopter Operating in a Turbulent Ship Airwake." *Journal of Aerospace Engineering – Proceedings of the Institute of Mechanical Engineers Part G*, Special issue on shipborne aviation, Vol. 219, November 2005, pp. 445-458.

[5]Wu, A. D., Johnson, E. N., and Proctor, A. A., "Vision Aided Inertial Navigation for Flight Control," AIAA Guidance, Navigation and Control Conference, San Francisco, California, August 2005.

[6]Langelaan, J. W., "State Estimation for Autonomous Flight in Cluttered Environments," *Journal of Guidance, Control and Dynamics*, Vol. 30, (5), September-October 2007, pp. 1414–1426.

[7]Holmes, W. K., and Langelaan, J. W., "Autonomous Ship-board Landing using Monocular Vision," AHS 72nd Annual Forum Proceedings, West Palm Beach, Florida, May 2016.

[8]Arora, S., Jain, S., Scherer, S., et. al. "Infrastructure-free Shipdeck Tracking for Autonomous Landing," 2013 IEEE International Conference on Robotics and Automation (ICRA) Proceedings, Karlsruhe, Germany, May 2013.

[9]Horn, J. F., He, C., Tritschler, J. K., et. al. "Autonomous Ship Approach and Landing using Dynamic Inversion Control with Deck Motion Prediction," 41st Annual European Rotorcraft Forum Proceedings, Munich, Germany, September 2015.

[10]Shin, H., You, D., and Shim, D. H., "Autonomous Shipboard Landing Algorithm for Unmanned Helicopters in Crosswind", *Journal of Intelligent & Robotic Systems*, Vol. 74, Issue 1-2, April 2014, pp 347-361. doi: 10.1007/s10846-013-9927-2

[11]Tritschler, J. K., Horn, J. F., and He, C., "Objective Function Development for Optimized Path Guidance for Rotorcraft Shipboard Recovery," Paper AIAA 2015-2395, AIAA Atmospheric Flight Mechanics Conference Proceedings, AIAA Aviation Forum, Dallas, TX, June 2015.

[12]Williams, G., Aldrich, A. and Theodorou, E. A., "Model Predictive Path Integral Control: From Theory to Parallel Computation," *Journal of Guidance, Control, and Dynamics*, Vol. 40, No. 2, Feb. 2017, pp. 344-357. doi: 10.2514/1G001921

[13]Prasad, J. V. R., Comandur, V., Walters, R., and Guerrero, D., "Model Predictive Path Integral Approach for Trajectory Guidance of Rotorcraft Shipboard Landing," AHS 74th Annual Forum Proceedings, Phoenix, Arizona, May 2018.

[14]FLIGHTLAB XAnalysis User Manual, Advanced Rotorcraft Technology, Inc., July 2013.

[15]Bryson Jr., A. E., and Ho, Y.-C., "Linear feedback to follow a desired output," *Applied Optimal Control: Optimization, Estimation and Control*, Chap. 5, CRC Press, New York, NY, 1975, pp. 175.

Presented at 44th European Rotorcraft Forum, Delft, The Netherlands, 19-20 September, 2018